

AD-A149 474

THE EFFECTS OF DENSE HOT PLASMAS ON ATOMIC SYSTEMS(U)
BERKELEY RESEARCH ASSOCIATES INC CA U GUPTA ET AL.
01 MAR 83 PD-BRA-83-288R DNA-TR-81-311 DNA001-81-C-0053

1/1

UNCLASSIFIED

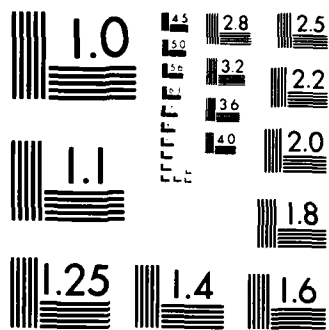
F/G 20/9

NL

END

FILMED

DTIC



MICROCOPY RESOLUTION TEST CHART
NATIONAL BUREAU OF STANDARDS 1963-A

AD-A149 474

12

DNA-TR-81-311

THE EFFECTS OF DENSE, HOT PLASMAS ON ATOMIC SYSTEMS

Uday Gupta
J.H. Orens
Berkeley Research Associates, Incorporated
P.O. Box 983
Berkeley, California 94710

1 March 1983

Technical Report

CONTRACT No. DNA 001-81-C-0053

APPROVED FOR PUBLIC RELEASE;
DISTRIBUTION UNLIMITED.

THIS WORK WAS SPONSORED BY THE DEFENSE NUCLEAR AGENCY
UNDER RDT&E RMSS CODE B323081466 T99QAXLA00013 H2590D.

Prepared for
Director
DEFENSE NUCLEAR AGENCY
Washington, DC 20305

DTIC
ELECTE
JAN 23 1985
S B

84 11 05 098

Destroy this report when it is no longer needed. Do not return to sender.

PLEASE NOTIFY THE DEFENSE NUCLEAR AGENCY,
ATTN: STTI, WASHINGTON, D.C. 20305, IF
YOUR ADDRESS IS INCORRECT, IF YOU WISH TO
BE DELETED FROM THE DISTRIBUTION LIST, OR
IF THE ADDRESSEE IS NO LONGER EMPLOYED BY
YOUR ORGANIZATION.



UNCLASSIFIED

SECURITY CLASSIFICATION OF THIS PAGE (When Data Entered)

REPORT DOCUMENTATION PAGE		READ INSTRUCTIONS BEFORE COMPLETING FORM
1. REPORT NUMBER DNA-TR-81-311	2. GOVT ACCESSION NO. AD-A149474	3. RECIPIENT'S CATALOG NUMBER
4. TITLE (and Subtitle) THE EFFECTS OF DENSE, HOT PLASMAS ON ATOMIC SYSTEMS		5. TYPE OF REPORT & PERIOD COVERED Technical Report
		6. PERFORMING ORG. REPORT NUMBER PD-BRA-83-288R
7. AUTHOR(s) Uday Gupta Joseph H. Orens		8. CONTRACT OR GRANT NUMBER(s) DNA 001-81-C-0053
9. PERFORMING ORGANIZATION NAME AND ADDRESS Berkely Research Associates, Inc. P.O. Box 983 Berkeley, California 94710		10. PROGRAM ELEMENT, PROJECT, TASK AREA & WORK UNIT NUMBERS Task T99QAXLA-00013
11. CONTROLLING OFFICE NAME AND ADDRESS Director Defense Nuclear Agency Washington, DC 20305		12. REPORT DATE 1 March 1983
		13. NUMBER OF PAGES 46
14. MONITORING AGENCY NAME & ADDRESS (if different from Controlling Office)		15. SECURITY CLASS. (of this report) UNCLASSIFIED
		15a. DECLASSIFICATION/DOWNGRADING SCHEDULE N/A since UNCLASSIFIED
16. DISTRIBUTION STATEMENT (of this Report) Approved for public release; distribution is unlimited.		
17. DISTRIBUTION STATEMENT (of the abstract entered in Block 20, if different from Report)		
18. SUPPLEMENTARY NOTES This work was sponsored by the Defense Nuclear Agency under RDT&E RMSS Code B323081466 T99QAXLA00013 H2590D.		
19. KEY WORDS (Continue on reverse side if necessary and identify by block number) Dense Plasmas Atomic Physics Plasma Polarization Equation-of-State		
20. ABSTRACT (Continue on reverse side if necessary and identify by block number) This report covers research into equation-of-state properties and plasma polarization effects produced by dense, hot plasmas on atomic systems. The work is part of a larger program to understand, simulate, and scale large X-ray sources under development by Defense Nuclear Agency.		

DD FORM 1473 1 JAN 73 EDITION OF 1 NOV 68 IS OBSOLETE

UNCLASSIFIED

SECURITY CLASSIFICATION OF THIS PAGE (When Data Entered)

PREFACE

It is a pleasure to thank Drs. J. Davis and M. Blaha for their active interest, useful suggestions and guidance throughout the course of this work. The overall guidance of Dr. J. Davis was of special value for this work. Dr. Blaha's help in the numerical work is gratefully acknowledged.

Accession For	
NTIS GRA&I	<input checked="" type="checkbox"/>
DTIC TAB	<input type="checkbox"/>
Unannounced	<input type="checkbox"/>
Justification	
By _____	
Distribution/	
Availability Codes	
Dist	Avail and/or Special
A-1	



TABLE OF CONTENTS

<u>Section</u>	<u>Page</u>
PREFACE	1
LIST OF ILLUSTRATIONS	3
1. INTRODUCTION	5
2. THE EQUATION-OF-STATE FOR DENSE, HOT PLASMAS	8
3. THE PLASMA POLARIZATION EFFECT	13
REFERENCES	18
APPENDIX I	
THE EOS-MODEL	19
APPENDIX IIA	
THE PLASMA POLARIZATION EFFECT	27
APPENDIX IIB	
HYDROGENIC IONS IN PLASMAS	31

LIST OF ILLUSTRATIONS

<u>Figure</u>		<u>Page</u>
1	Electronic contribution to the EOS in the temperature range 0 - 100 eV and the density range 10^{20} - 10^{24} electrons/cm ² .	37
2	Total electronic exchange-correlation contribution to the thermodynamic potential Ω as a function of temperature for two different electronic densities.	38
3	The exchange-correlation potential $V_{xc}[n,T]$ for electrons scaled by their zero temperature value $V_{xc}[n,0]$ as a function of electron density at three typical plasma temperatures.	39
4	The strong density dependence of the self-consistent atomic potential Eq. (II-9) for a Neon ion embedded in a hydrogen plasma at $T = 200$ eV.	40
5	Energy-level spectrums for a Neon ion in a hydrogen plasma.	41

SECTION 1
INTRODUCTION

Equation of state data (pressure, total energy, specific heat and other thermodynamic properties) for plasmas in a wide range of conditions is a problem area of considerable importance. For a low density fully ionized plasma at very high temperatures, classical EOS-results are available and are generally valid. However, EOS-properties for high density, low temperature plasmas (including the "cold" compressed matter phase) are much more complicated, particularly for partially ionized conditions. In this domain, available EOS-data is scanty, and, in cases where it is available, the models¹ used do not adequately take into account the physics of the interacting plasmas. This is particularly true for the electronic contribution to the EOS. Depending on the density and temperature, quantum effects are very significant for electron-electron and electron-ion interactions. At intermediate densities and temperatures, plasmas can be "strongly coupled" as well as partially ionized. Both of these aspects need careful consideration and have not been properly included in previous models. In addition, for improved accuracy, the "cold" compressed matter phase needs consideration of solid-state effects.

Plasmas in the above-mentioned conditions occur in a variety of experimental conditions--shock-compressed materials, the superdense core of laser-fusion plasmas, laser-imploded solid targets or multi-layered materials, etc. The ongoing research on these processes requires a knowledge of the appropriate EOS-properties. Improved EOS-data is also needed for more realistic hydrodynamical

calculations (including radiation transport), for studying implosion characteristics of cylindrical radiating plasmas, as well as for a variety of atomic calculations.

This need motivated a more realistic EOS-model suitable for a wide range of plasma conditions, densities and temperatures. The present report provides such a comprehensive EOS-model, justifies the theoretical basis and presents numerical results obtained. This model is based on the density functional method² generalized to arbitrary temperatures. This method enables a systematic incorporation of the above-mentioned effects. In Section 2, physical considerations for this model are outlined, its theoretical basis is justified and the implications of the numerical results are discussed. The specific mathematical details of the scheme are given in Appendix I.

In Section 3, research on problems involving polarization shifts in dense, hot plasmas is presented. This is an important effect that affects atomic processes in plasmas, particularly the radiation characteristics. These atomic processes involve consideration of the number and spacing of ionic energy levels, level populations, transition probabilities, etc. These parameters as well as radiation transport through hot plasmas are known to be drastically affected by a dense plasma environment. The plasma polarization shift (PPS) plays a significant role in this context. The dense plasma environment produces significant lowering of the ionization potential which can eliminate excited atomic energy levels and possibly entire stages of ionization. Although previous work has been done to include this "lowering" in atomic calculations¹, the majority of these models are semi-

empirical. Detailed investigation of the PPS over a wide range of plasma densities and temperatures is important for understanding the radiation characteristics of hot plasmas as well as for a variety of atomic calculations.

A systematic study of plasma polarization effects is outlined in Section 3. Our model is discussed and compared with other commonly used static screening models. The improvements of the present model are that it treats nonlinear screening effects exactly and quantum many-body effects are included via a self-consistent scheme. This model is applied to Neon and Argon impurities in dense, hot plasmas and results are compared with those from the Debye-Hückel model. Drastic differences in the energy-level structure indicate the usefulness of this nonlinear self-consistent model for dense plasmas where Debye-Hückel-type models are inadequate.

For purposes of plasma diagnostics, specific ionization stages (or ionic species) need to be considered. A scheme suitable for application in a wide range of plasma conditions is examined. Connections are made to the nonlinear screening model mentioned previously. Implementation of a computer code incorporating the above algorithm is currently in progress. This should provide DNA with a suitable data base for a variety of atomic calculations in dense, hot plasmas.

SECTION 2

THE EQUATION-OF-STATE FOR DENSE, HOT PLASMAS

In developing a theoretical model for the computation of equation-of state (EOS) data and other thermodynamic properties of plasmas over a wide range of densities and temperatures, one is faced with the task of properly describing the physics of vastly different system conditions and properties. In the low density, high temperature region, the plasma is "weakly coupled"--that is, the random thermal motion dominates over the Coulomb interaction between charged plasma particles. In this region, many-body field theoretic methods can be used to obtain the EOS-data. However, for high densities and low temperatures (as obtained for shock-compressed materials, the superdense core of laser-fusion plasmas, laser-imploded solid targets, etc.), the plasma is in the "strongly-coupled" condition. Coulomb interaction dominates over the thermal motion of the plasma particles and perturbative methods are no longer applicable.

In this context, the local density functional scheme of Kohn and Sham³, generalized to arbitrary temperatures by us², offers a very useful and practical method of calculation of EOS-data. We have developed such a scheme for two-component systems with arbitrary coupling conditions applicable to both pure plasmas (partially ionized Aluminum, for example) as well as for plasmas seeded with impurity ions.

In this density functional method (DFT), the charge-density profiles of ions and electrons of the inhomogeneous plasma play a central role. In a partially ionized plasma

at an arbitrary density and temperature, the positive ion-centers form an attractive potential for the electrons--some forming bound states, others occupying continuum states. In the DFT, both the bound and continuum states are treated quantum-mechanically via solution of the Schrödinger equation. This, in turn, accounts for a significant improvement over other semi-classical approximations commonly used for plasma calculations¹. The effective potential in the DFT contains, aside from the nuclear and electrostatic terms, an exchange-correlation contribution arising from Coulomb interactions between charged particles. The appropriate degeneracy effects are maintained through Fermi-Dirac statistics for the electrons. The electronic charge-densities are constructed from the probability densities obtained from the wave functions and are weighted by the occupation probabilities of the various electronic states according to F-D statistics. The effective potential is then constructed from the charge density profiles (with its associated exchange-correlation potential) and the procedure iterated to self-consistency. The self-consistent electron and ion charge density profiles are used to calculate various thermodynamic properties and EOS-data (pressure, total energy, specific heat, etc.). The mathematical details of the scheme are given in Appendix I.

At this point, the following aspects of the scheme should be noted:

1. The well-known inadequacies of the Thomas-Fermi method^{1,4}, extensively applied for EOS-calculations, are removed. That is, the kinetic energy is treated exactly and, unlike the Thomas-Fermi method, the exchange-correlation effects are included.

2. The exchange-correlation potential V_{xc} needed in this scheme can be calculated by many-body theory techniques. This has been developed and the relevant Feynman diagrams computed numerically^{5,6}. These quantities are thus readily available for use in the above algorithm.

3. Through the effective potential, the scheme also provides the correct dielectric function for the plasma. In strongly-coupled plasmas, the usual mean-field approximations are no longer valid. Thus, complicated nonlinear methods are needed to calculate the plasma dielectric function. Moreover, the present scheme is equally valid for strongly as well as weakly-coupled plasmas. The dielectric functions obtained through this scheme can be used for a variety of plasma calculations (energy loss of fast-charged particles moving through the plasma, pair distribution functions and structure factors, bulk thermodynamic properties, etc.).

In the "weakly coupled" domain, it is simpler to use many-body field theoretic methods to calculate EOS-data. The ionic and the electronic contributions can be separated as a first approximation and evaluated individually. Except for very low temperatures, the electronic contributions dominate the overall EOS-properties. At a given density and temperature, the interacting electron system pressure (or total energy) can be calculated by evaluating the kinetic energy part exactly and the interaction energy part through a many-body perturbation method. The first order exchange term, arising from the Pauli exclusion principle, is purely quantum-mechanical in nature. The correlation energy is evaluated in this scheme via numerical summation of the relevant Feynman (ring) diagrams.

The "ring" diagram sum is known to yield the Gell-Mann and Brueckner⁸ result in the degenerate limit and goes over to the Debye value for the correlation energy⁹ in the non-degenerate (classical) limit. Thus they are expected to interpolate properly through the intermediate degeneracy region. The mathematical details are given in Appendix I.

The numerical results for the electronic pressure obtained from this scheme for electron densities $10^{24} - 10^{20} \text{ cm}^{-3}$ and temperatures 0 - 10 eV are given in Table 1. The drastic difference from the ideal gas EOS are illustrated in Figure 1. The differences progressively reduce with decreasing density and increasing temperature, but even for a density as low as 10^{20} cm^{-3} and a temperature of 1 eV ($\approx 10,000^\circ\text{K}$), the difference is still more than 50%. This shows that the ideal gas EOS is not valid in this density-temperature range. At high density and low temperatures the exchange effect dominates the interaction energy, whereas in the moderate density and temperature ranges, the correlation energy is more important. As the temperature increases, the very slow rise of the pressure-curve for a fixed density is because the increase in the correlation contribution is partly offset by the decrease in the exchange effect.

These results indicate that there exists a wide range of densities and temperatures where systematic investigations of the EOS-properties are needed to avoid drastic errors in the data. Even in the weakly-coupled domain, many-particle effects are very substantial. For strongly-coupled plasmas, ion-ion and ion-electron interactions are important in addition to electronic contributions. Partially ionized plasma conditions present further

complications. The model outlined here incorporates these effects in a systematic way. The computer code being developed based on this algorithm is expected to provide accurate EOS-data over a wide range of plasma conditions.

SECTION 3

THE PLASMA POLARIZATION EFFECT

The screening of a static external charge immersed in a plasma has been of central importance not only in plasma physics but also in astrophysics and semi-conductor physics. Traditionally the static screening has been described in terms of a shielded potential of the form $V_s(r) = \frac{Z}{r} e^{-r/\lambda}$ (λ is the screening parameter). Debye Hückel and Thomas-Fermi-type models fall under this category. Physically the electric field of the external charge polarizes the surrounding medium so that unlike charges pile up around the external charge whereas like charges are repelled from it. This results in modifying the bare Coulomb potential to a "screened" potential. A simple approximate form of the screened potential is given by V_s .

A general approach to the plasma polarization effect can be made via an appropriate dielectric response function. In general, this approach leads to complicated nonlinear methods¹⁰ which are very difficult to apply to plasma problems. Within linear response theory, however, the random phase (RPA) dielectric function provides a useful, practical approach.

In recent years, the RPA dielectric function was generalized to arbitrary temperatures and densities and a more complete analysis of static screening was done¹¹. This analysis showed that the effective screened potential goes over to the Debye potential in the high temperature, low density region and to the Thomas-Fermi potential in the low temperature, high density region. The RPA-screened

potential thus provides a natural way to interpolate between these two limits and provides a scheme to investigate the screening effects in the intermediate range of densities and temperatures. Here neither the Debye nor T-F model is applicable. If the temperature of the plasma is of the order of the Fermi temperature, T_F , drastic differences were obtained in the level spectrum calculated using the RPA-screened potential as compared to the spectrum obtained from the Debye potential. Degeneracy effects and a correct momentum dependence account for these differences. This is illustrated in Table 2.

Within linear response theory, the RPA-screened potential describes the screening effects better than the Debye or T-F models. The linear response theory, however, underestimates the charge pile-up around the ions. This produces smaller screening shifts of the ionic energy levels than would be obtained from a more accurate model. A full nonlinear self-consistent model is therefore required for appropriate treatment of screening effects. The model we have developed treats the nonlinear screening effects exactly. The correct charge density profile around an ion is constructed from the probability densities obtained from the wave functions and is weighted by the occupation probabilities of the various electronic states according to Fermi statistics. The effective atomic potential contains, aside from the nuclear and electrostatic terms, an exchange-correlation contribution arising from the Coulomb interactions between charged particles. These last two quantities depend on the effective atomic potential via solution of the Schrödinger equation. The procedure is iterated to self-consistency. Such a numerical calculation is approximately ten times faster

than a self-consistent Hartree-Fock calculation. The model has the merit of treating the screening effect exactly and the many-body effects in an adequate way.

Our model was applied to Neon and Argon impurities in a dense, hot hydrogen plasma. At the chosen temperature and density ($T = 200$ eV, $n_e \sim 10^{23} - 10^{24}$ cm⁻³), hydrogen is fully ionized. A comparison of the results (Table 3) of the self-consistent calculation with those from the Debye model show that the energy levels obtained through the Debye potential are drastically deeper than the self-consistent spectrum. This is because the linear screening model (Debye-Hückel) underestimates the charge pile-up around the ion. The correct charge density profile is obtained from the self-consistent potential which, in turn, produces larger screening shifts. The other consequence of this effect is that the Debye potential incorrectly predicts a larger number of bound states. Also, the line shifts obtained in the Debye model are substantially different from the self-consistent model results. This is important because the bound-bound transition probability varies as the cube of the level separation. The usefulness of our model, which yields the correct screening effect in dense, hot plasmas, is therefore obvious.

The existence of different ionic species (hydrogenic, helium-like, etc.) in experimentally observed spectra from hot plasmas is an additional aspect that needs to be considered. For determination of the correct energy-level spectrum of one-, two- or multi-electron ions in hot plasmas, the above model needs to be extended. For purposes of illustration, the case of a 1-electron hydrogen-like ion immersed in hot plasma is considered

in Appendix IIB. For most practical purposes, the 1-electron spectrum is within a few percent of the level spectrum obtained in the self-consistent calculation discussed above.

Previous calculations by Skupsky¹² and by Davis and Blaha¹³ utilize two different approaches to the problem of a 1-electron spectrum in dense, hot plasmas. Davis and Blaha¹³ employ an approach similar to a self-consistent Hartree-Fock method and leave out the self-interaction term from the screened potential. Also, the exchange-correlation potential was included only for the continuum electrons and not for the bound electrons. Calculations were done for level shifts, coefficients of transition probabilities, and electron collision cross-sections of: Ne^{9+} for temperatures 200 - 500 eV and electron densities $(1 - 6) \times 10^{24} \text{ cm}^{-3}$; and Ar^{7+} for temperatures 1000 - 2000 eV and electron densities $(2 - 8) \times 10^{25} \text{ cm}^{-3}$. The general trends of the results indicate substantial screening effects on those atomic parameters.

In his scheme, Skupsky¹² solves Poisson's equation self-consistently to obtain an effective potential which includes both bound and free electrons. However, the free-electron density is evaluated in a semi-classical approximation and many-body effects were neglected. In contrast, our model constructs the free electron charge density via solution of the Schrödinger equation and includes exchange-correlation effects.

In conclusion, we note that our model treats the nonlinear screening effect in an exact fashion and the many-body effects adequately. For plasmas in the intermediate degeneracy region, as occurs in the dense core of laser fusion plasmas, shock-compressed material at

elevated temperatures, etc., this model can readily be applied to investigate screen effects on atomic parameters. For multi-electron ions in plasmas, however, this model needs to be extended. Currently we are in the process of developing such a model. This will provide an important diagnostic tool.

REFERENCES

1. For a recent review of such models, see for example, R. More, U.C.R.L. - 84991 (1981).
2. U. Gupta and A.K. Rajagopal, Review Article in Physics Reports. Vol. 87, No. 6 (1982).
3. W. Kahn and L.J. Sham, Phys. Rev. 140, A1133 (1965).
N.D. Mermin, Phys. Rev. 137, A 1441 (1965).
4. R.D. Cowan and J. Ashkin, Phys. Rev. 105, 144 (1957).
5. U. Gupta and A.K. Rajagopal, Phys. Rev. A22, 2064, (1980).
6. M.W.C. Dharma-Wardana and R. Taylor, J. Phys. C2, 876 (1981).
7. U. Gupta and A.K. Rajagopal, J. Phys. B14, 2309 (1981).
8. M. Gell-Mann and K.A. Brueckner, Phys. Rev. 106, 364 (1957).
9. E.W. Montroll and J.C. Ward, Phys. Fluids 1, 55 (1958).
10. Several different approaches on nonlinear methods are available: P. Vashista and K.S. Singwi, Phys. Rev. B6, 875(1972), H. Totsuji and S. Ichimaru, Prog. Theor. Phys. 52, 42 (1974) and references therein.
11. U. Gupta and A.K. Rajagopal, J. Phys. B12, L703 (1979).
12. S. Skupsky, Phys. Rev. A21, 1316 (1980).
13. J. Davis and M. Blaha, Article in Physics of Electronics and Atomic Collisions (North Holland), 911 (1982).

APPENDIX I
THE EOS-MODEL

In this section, we will outline our EOS-model and the method of calculation. Consider a partially ionized plasma (say Aluminum or Argon) at a given density and temperature. Because of the polarization effect, electrons will tend to pile up around the ions--some forming bound states, others occupying continuum states. Considering a central ion, the other positive ions will be repelled from it whereas electrons will be attracted. A sphere of radius R around the central ion will be electrically neutral, i.e.

$$Z - \int_{r \leq R} \rho_e(\vec{r}) d\vec{r} + Z \int_{r \leq R} \rho_p(\vec{r}) d\vec{r} = 0 \quad (\text{I-1})$$

where $\rho_e(r)$ and $\rho_p(r)$ are the electron and ion density profiles around the central ion. Note that Eq. (I-1) really defines the radius R . If n_b is the mean number of electrons bound to the central ion,

$$\bar{Z} = Z - n_b \quad (\text{I-2})$$

represents the average charge per ion. n_b is defined by integrating the R.H.S. of Eq. (I-8g) over all r . According to density functional theory, the thermodynamic potential Ω of the system is uniquely determined if the correct density distributions $\rho_e(r)$ and $\rho_p(r)$ are known:

$$\Omega = T \left[\rho_e, \rho_p \right] + \Omega_e + \Omega_i + \Omega_{ei} \quad (\text{I-3})$$

where $T[\rho_e, \rho_p]$ is the kinetic energy sum of ions and electrons, and

$$\Omega_e = -\int \frac{Z}{r} \rho_e(\vec{r}) d\vec{r} + \frac{1}{2} \int \frac{\rho_e(\vec{r}) \rho_e(\vec{r}') d\vec{r} d\vec{r}'}{|\vec{r} - \vec{r}'|} + \int F_{xc}^e \rho_e d\vec{r} - \mu_e \int \rho_e(\vec{r}) d\vec{r} \quad (I-4)$$

$$\Omega_i = \bar{Z} \int \frac{Z}{r} \rho_p(\vec{r}) d\vec{r} + \frac{\bar{Z}^2}{2} \int \frac{\rho_e(\vec{r}) \rho_e(\vec{r}') d\vec{r} d\vec{r}'}{|\vec{r} - \vec{r}'|} + \int F_c^i \rho_p d\vec{r} - \mu_i \int \rho_p(r) dr \quad (I-5)$$

$$\Omega_{ei} = -\bar{Z} \int \frac{\rho_e(\vec{r}) \rho_p(\vec{r}') d\vec{r} d\vec{r}'}{|\vec{r} - \vec{r}'|} + \int F_c^{ei} \rho_e, \rho_p d\vec{r} \quad (I-6)$$

In the above, F_{xc}^e is the exchange-correlation free energy of the electrons and μ_e is the electron chemical potential. The exchange free energy of ions is negligible. Therefore only the correlation part F_c^i is retained. To simplify calculations, we will neglect F_c^{ei} which is negligibly small in most cases of interest.

To take into account the charge-neutrality condition (I-1), we consider the quantity

$$\Omega_T = \Omega - \lambda \left[Z + \bar{Z} \int_R \rho_e(r) dr - \int_R \rho_p(\vec{r}) d\vec{r} \right] \quad (I-7)$$

where λ is Lagrange multiplier. The stationary condition of Ω_T leads to the following system of equations for the electrons and ions to be solved self-consistently:

$$\left[-\frac{\nabla^2}{2} - \frac{Z}{r} + \int \frac{[\rho_e(\vec{r}') - \bar{Z} \rho_p(\vec{r}')] d\vec{r}'}{|\vec{r} - \vec{r}'|} + v_{xc}^e(r, \rho_e, T) - \mu_e + \lambda \right] \psi_i(r) = \epsilon_i \psi_i(r) \quad (I-8)$$

with

$$\rho_e(r, T) = \sum_i |\psi_i(r)|^2 \frac{1}{\left[e^{\beta(\epsilon_i - \mu_e)} + 1 \right]} \quad (\text{I-8a})$$

(the sum over i involves the sum over bound and continuum states) and $V_{xc}^e = \delta F_{xc}^e / \delta \rho_e(r)$ is the exchange-correlation potential for the electrons.

For the ions, we get a similar set of equations:

$$\left[\frac{-\nabla^2}{2} + \frac{\bar{Z}Z}{r} - \bar{Z} \int \frac{[\rho_e(\vec{r}') - \bar{Z}\rho_p(\vec{r}')] d\vec{r}'}{|\vec{r} - \vec{r}'|} + V_c^i(r) - \mu_p - Z\lambda \right] \phi_i(r) = \epsilon_i \phi_i(r) \quad (\text{I-9})$$

Due to their heavier mass, the ions form a classical subsystem for most cases of interest. Hence the ion charge density distribution can be well represented by

$$\rho_p(r) = e^{\beta \mu_i} \exp \left[-\beta V_i(r) \right] \quad (\text{I-9b})$$

where $\mu_i = \mu_i - V_c^i(R) + \bar{Z}\lambda$

$$\text{and } V_i(r) = \bar{Z} \left[\frac{Z}{r} - \int \frac{[\rho_e(\vec{r}') - Z\rho_p(\vec{r}')] d\vec{r}'}{|\vec{r} - \vec{r}'|} \right] + V_c^i(r) - V_c^i(R) \quad (\text{I-9c})$$

The calculation thus reduces to obtaining the correct density distributions $\rho_e(r, T)$ and $\rho_p(r, T)$ self-consistently.

$$\text{Defining } \bar{\mu}_e = \mu_e - V_{xc}^e(R) - \lambda \quad (\text{I-8b})$$

Eq. (I-8) is cast into the form

$$\left[-\frac{\nabla^2}{2} + \bar{V}_{\text{eff}}^e(r, \rho_e, T) \right] \psi_i(r) = \epsilon_i \psi_i(r) \quad (\text{I-8d})$$

$$\text{with } \bar{V}_{\text{eff}}^e(r, \rho_e, T) = -\frac{Z}{r} + \int \frac{[\rho_e(\vec{r}') - Z\rho_p(\vec{r}')] d\vec{r}'}{|\vec{r} - \vec{r}'|} + V_{xc}^e(r) - V_{xc}^e(R) \quad (\text{I-8e})$$

The electron density distribution is the sum of bound and continuum state contributions:

$$\rho_e(r) = \rho_e^b(r) + \rho_e^c(r) + \rho(R) \quad (\text{I-8f})$$

$$\text{where } \rho_e^b(r) = \sum_{i, \ell} 2(2\ell+1) |\psi_{i\ell}(r)|^2 f(\epsilon_i, \bar{\mu}_e) \quad (\text{I-8g})$$

$$\rho_e^c(r) = \frac{1}{\pi^2} \int_0^\infty dk k^2 f(k, \bar{\mu}_e) \sum_{\ell} (2\ell+1) \left[\psi_{k\ell}^2(r) - j_{k\ell}^2(r) \right] \quad (\text{I-8h})$$

$\rho(R)$ is effectively the bulk electron density ρ_0 and the j 's are spherical Bessel functions. In actual calculations, it is convenient to work with $\bar{\mu}_e$, $\rho(R)$ and the mean density $\bar{\rho}$. That is, we can start off with a given mean electron density $\bar{n}_e = \bar{Z} \bar{\rho}$ and a chemical potential $\bar{\mu}_e$ and adjust $\rho(R)$ to ensure electrical neutrality.

Once the electron and ion charge density distributions $\rho_e(r, T)$ and $\rho_p(r, T)$ are calculated self-consistently, all the thermodynamic quantities can be readily obtained. For example, the pressure P of the plasma is given by

$$P = -R/V, \quad (I-10)$$

(V = Volume), with R obtained from Eq. (I-3) at any density and temperature. The total energy E of the plasma is given by

$$E = R + \mu_e N_e + \mu_p N_p + TS \quad (I-11)$$

where the entropy S is obtained from the set of eigenvalues ϵ_i 's and the occupation probabilities f_i 's already computed;

$$S = \sum_i \left[f_i \ln f_i + (1-f_i) \ln(1-f_i) \right] \quad (I-12)$$

For hydrodynamic calculations, several other quantities like $(dE/d\rho)$, $(dP/d\rho)$, (dP/dT) etc. are needed. These again, are readily obtained from knowledge of the total energy E and pressure P.

MANY-BODY PERTURBATION METHOD

As mentioned in Section 2, the above scheme is particularly applicable for strongly-coupled plasmas. However, in the weakly-coupled domain, it is simpler to use many-body perturbation theory to calculate EOS-data. This is discussed below. Of particular importance is the electronic contribution to the EOS. Let us focus our attention to an interacting electron system of density ρ at a temperature T. The thermodynamic potential $\Omega[\rho, T]$ can be written as

$$\Omega[\rho, T] = \Omega_0 + \Omega_{xc} \quad (I-13)$$

where Ω_0 is the non-interacting part

$$\frac{\rho_0}{V} = -2 \int_0^{\infty} dx x^4 \frac{1}{\left[e^{(t^{-1}x^2 - \alpha)} + 1 \right]} \quad (\text{I-14})$$

with $\epsilon_F = \hbar^2 (3^{-2} \rho_0)^{2/3} / 2m$, the Fermi energy of the electrons, $x = k/k_{\text{Fermi}}$, and $\alpha = \mu/K_B T$ is the degeneracy parameter. For arbitrary densities and temperatures, α is to be determined from the phase space integral,

$$\frac{1}{3} = \int_0^{\infty} dx \frac{x^2}{\left[e^{(t^{-1}x^2 - \alpha)} + 1 \right]} \quad (\text{I-15})$$

($t = T/T_{\text{Fermi}}$). At zero temperature

$$\frac{\rho_0}{V} (T=0) = \frac{2}{5} \rho_0 \epsilon_F \quad (\text{I-14a})$$

with the corresponding pressure

$$P_0 (T=0) = \frac{2}{5} \rho_0 \epsilon_F$$

At high temperatures, $T \rightarrow \infty$, one recovers the ideal gas equation of state

$$P_0 \xrightarrow{T \rightarrow \infty} \rho_0 K_B T \quad (\text{I-14b})$$

The interaction part of the thermodynamic potential $\Omega_{xc}[\rho, T]$ is a difficult many-body quantity. The exchange part arises from the Pauli exclusion principle whereas the correlation effects arise from the Coulomb repulsion between electrons which tend to keep them apart. The leading exchange contribution Ω_x is

$$\frac{\Omega_x}{V} = -\frac{e^2 (3\pi^2 \rho)^{4/3}}{4\pi^3} \cdot 2 \int_0^\infty \int_0^\infty dx dy \frac{xy}{\left[e^{(t-1)x^2-t} + 1 \right] \left[e^{(t-1)y^2-t} + 1 \right]}{\ln \left| \frac{x+y}{x-y} \right|} \quad (\text{I-16})$$

At zero temperature, we have

$$\frac{\Omega_x(T=0)}{V} = -\frac{e^2}{4\pi^3} (3\pi^2 \rho)^{4/3} \quad (\text{I-16a})$$

whereas, in the high temperature limit, $T \rightarrow \infty$

$$\frac{\Omega_x(T \rightarrow \infty)}{V} = -\frac{e^2}{4\pi^3} (3\pi^2 \rho)^{4/3} \frac{4\epsilon_F}{9K_B T} \quad (\text{I-16b})$$

Since in the weakly-coupled regime, the interaction is small compared to the average kinetic energy, diagrammatic perturbation theory can be used to calculate the correlation energy. The "ring" diagram sum gives the correlation contribution:

$$\frac{\Omega_c(r)}{V} = \frac{K_B T}{2} \int \frac{d^3 q}{(2\pi)^3} \sum_{\nu_n} \left\{ \ln \left[1 - \frac{4\pi e^2}{q^2} \chi(q, \nu_n) \right] + \frac{4\pi e^2}{q^2} \chi(q, \nu_n) \right\} \quad (\text{I-17})$$

where the polarization function is

$$\chi(q, \nu_n) = -2 \int \frac{d^3 p}{(2\pi)^3} \frac{f(p+q) - f(p)}{i\hbar \nu_n - (\epsilon_{p+q} - \epsilon_p)} \quad (\text{I-17a})$$

with $\nu_n = 2n\pi K_B T / \hbar$, ($n = \text{integers}$). $f(p)$ is the Fermi function. In the high temperature limit, most of the

contribution comes from the static part ($v_n = 0$) of Eq. (I-17) and from the small momentum transfers ($q \rightarrow 0$). In this $T \rightarrow \infty$ limit,

$$\frac{\Omega_c(r)}{V} \xrightarrow{T \rightarrow \infty} -\frac{2}{3} \sqrt{\pi} \frac{e^3 \rho^{3/2}}{(K_B T)^{1/2}} \quad (\text{I-17b})$$

which is the usual Debye contribution to the correlation energy. At the opposite limit of zero temperature and very high densities, one obtains the well-known Gell-Mann and Brueckner result.⁸

APPENDIX IIA

THE PLASMA POLARIZATION EFFECT

Let us consider a homogeneous plasma of density n at a temperature T . If an external impurity charge $+Ze$ is immersed in the plasma, it will polarize the medium and bring about a redistribution of charge density. Within linear response theory, the effective potential $V_{\text{eff}}(r)$ at a distance r from the static impurity charge $+Ze$ is given by

$$V_{\text{eff}}(r, n, T) = -\frac{2Ze^2}{\pi} \int_0^{\infty} dq \left[\frac{\sin(qr)}{qr} \right] \frac{1}{1 - \frac{4\pi e^2}{q^2} \chi(q, n, T)} \quad (\text{II-1})$$

where $\chi(q, n, T)$ is an appropriate density and temperature dependent response function. The random phase form (RPA) of $\chi(q, n, T)$ generalized to arbitrary temperature gives

$$\frac{4\pi e^2}{q^2} \chi(q, n, T) = -\left(\frac{4k_F}{\pi a_0} \right) \frac{1}{q^3} \int_0^{\infty} dk k f(k) \ln \left| \frac{q+2k}{q-2k} \right| \quad (\text{II-2})$$

where q and k are momentum variables, $f(k)$ is the Fermi function, and k_F is the Fermi momentum; $k_F = (3\pi^2 n)^{1/3}$.

V_{eff} satisfies the consistency condition that the total induced charge density must compensate the external charge,

$$e \int d^3r \delta n_{\text{ind}}(r) = +Ze \quad (\text{II-3})$$

Unlike the Thomas-Fermi theory, this induced charge density is finite everywhere, including the origin.

One can show that the $q \rightarrow 0$ limit of Eq. (II-1) is the static screened Coulomb potential (SSCP):

$$V_{\text{eff}}(r, n, T) \xrightarrow{q \rightarrow 0} - \frac{Ze^2}{r} e^{-r\xi(n, T)} \quad (\text{II-4})$$

where the parameter ξ is defined by

$$\xi^2(n, T) = \xi_{\text{TF}}^2 \int_0^\infty dk f(k); \quad \xi_{\text{TF}}^2 = \frac{4k_F}{\pi a_0} \quad (\text{II-5})$$

Further, as $T \rightarrow \infty$, Eq. (II-1) yields the Debye-Hückel potential

$$V_{\text{eff}}(r, n, T) \xrightarrow[\substack{q \rightarrow 0 \\ T \rightarrow \infty}]{} - \frac{Ze^2}{r} e^{-r\xi_D}; \quad \xi_D^2 = \frac{4\pi n e^2}{k_B T} \quad (\text{II-6})$$

In the opposite limit of $T = 0$, one obtains the T-F screened potential

$$V_{\text{eff}}(r, n, T) \xrightarrow[\substack{q \rightarrow 0 \\ T=0}]{} - \frac{Ze^2}{r} e^{-r\xi_{\text{TF}}} \quad (\text{II-7})$$

Thus, the Debye and the Thomas-Fermi screening lengths are seen to be limiting forms of the generalized screening parameter $\xi(n, T)$ which contains the appropriate degeneracy effects. The full momentum (q) dependence of $V_{\text{eff}}(r)$ in Eq. (II-1) yields a further difference from the Debye or the T-F potential.

Level shifts of bound electronic energy levels, supported by an attractive impurity potential in a plasma, has been investigated extensively. The radiation from electronic transitions between these shifted energy levels is used as a plasma diagnostic. The problem requires the solution of the Schrödinger equation

$$\left(-\frac{\hbar^2}{2m} \frac{d^2}{dr^2} + \frac{\ell(\ell+1)\hbar^2}{2mr^2} + V_{\text{eff}}(r, n, T) \right) R_{n\ell}(r) = \epsilon_{n\ell} R_{n\ell}(r) \quad (\text{II-8})$$

where $R_{n\ell}(r)$ represents the radial part of the electron wave function with energy eigenvalue $\epsilon_{n\ell}$. Many previous¹ calculations have used the Debye potential in Eq. (II-8). Our results utilizing the R.P.A. screened potential in Eq. (II-8) and obtaining the energy levels by numerical solution of the Schrödinger equation is given in Table 2.

The linear screening method, however, underestimates the charge pile-up around a given ion. A full treatment therefore requires a nonlinear self-consistent method to investigate plasma screening effects. We will illustrate our method for the general case of a partially ionized plasma at an arbitrary temperature T .

If $\rho_e(r, T)$ and $\rho_p(r, T)$ represent the appropriate electron and ion density profiles, then the requirement of self-consistency implies the following set of coupled equations:

$$\left[-\frac{\nabla^2}{2} - \frac{z}{r} + \int \frac{[\rho_e(\vec{r}', T) - z\rho_p(\vec{r}', T)] d\vec{r}'}{|\vec{r} - \vec{r}'|} + V_{xc}^e(r, T) \right] \psi_i(r) = \epsilon_i \psi_i(r) \quad (\text{II-9})$$

$$\text{with } \rho_e(r, T) = \sum_i |\psi_i(r)|^2 \frac{1}{e^{\beta(\epsilon_i - \mu)} + 1} \quad (\text{II-10})$$

(the sum over i implies the sum over bound and continuum states), and,

$$\left[-\frac{\nabla^2}{2} + \frac{\bar{z}z}{r} - \bar{z} \int \frac{[\rho_e(\vec{r}', T) - z\rho_p(\vec{r}', T)] d\vec{r}'}{|\vec{r} - \vec{r}'|} + V_c^i(r) \right] \phi_i(r) = \epsilon_i \phi_i(r) \quad (\text{II-11})$$

In the above, $V_{xc}^e(r,T)$ is the exchange-correlation potential for electrons, $V_c^i(r)$ is the correlation potential, and \bar{Z} is the effective charge of a partially ionized ion. In most practical cases of interest the ions can be treated classically because of their heavier mass. Thus the solution of Eq. (II-1) becomes:

$$\rho_p(r,T) = \rho_o e^{-\beta V_i(r)} \quad (II-12)$$

with

$$V_i(r) = \bar{Z} \left[\frac{Z}{r} - \int \frac{[\rho_e(\vec{r}',T) - \rho_p(\vec{r}',T)] d\vec{r}'}{|\vec{r} - \vec{r}'|} \right] + V_c^i(r) \quad (II-13)$$

In setting up the above equation many-body effects have been included via $V_{xc}^e(r,T)$ for the electrons and V_c^i for the ions. Note that the induced charge displacement does compensate the nuclear charge over a large distance, thus accounting for complete screening. The above method was applied to Neon and Argon impurities in a fully ionized hydrogen plasma. The results are shown in Tables 3(a) and 3(b).

APPENDIX IIB

HYDROGENIC IONS IN PLASMAS

For purpose of illustration, we consider the specific case of a hydrogen-like ion (i.e., an ion with a single electron bound to it) in a plasma. (The extension to multi-electron ions is straightforward but the details will not be given here). A rigorous approach would require the self-consistent solution of a non-local integro-differential equation of the following form:

$$\left[-\frac{\nabla^2}{2} - \frac{Z}{r} + \int \frac{\rho(\vec{r}', T) d\vec{r}'}{|\vec{r} - \vec{r}'|} + \sum_j \int d\vec{r}' \sum (r, r', E) \phi_j(r') \right] \phi_i(r) = \epsilon_i \phi_i(r)$$

where $\sum (r, r', E)$ is the non-local, energy-dependent "mass" operator which involves knowledge of $\{\epsilon_j, \phi_j(r)\}$, the energy-levels, and the orbitals of interest. The following scheme substantially reduces the complexity of such a calculation while still retaining most of the many-body effects.

Let $\phi_{n\ell}(r)$ be the bound-state wave function of the electrons bound to the ion Z . $\phi_{n\ell}(r)$ could be any of the $1s, 2s, 2p \dots$ sequence of states. Based on physical considerations, we invoke the argument that the screening term affecting the bound electron does not include the part associated with the bound electron itself. In other words, we exclude the self-interaction effect. The energy level spectrum is then determined by the solution of

$$\left\{ -\frac{\nabla^2}{2} - \frac{z}{r} + \int \frac{[\rho(\vec{r}', T) - |\phi_{n\ell}(\vec{r}')|^2]^2 d\vec{r}'}{|\vec{r} - \vec{r}'|} + v_{xc}[\rho(r, T), T] \right. \\ \left. - v_{xc}[|\phi_{n\ell}(r)|^2, T] \right\} \phi_{n\ell}(r) = \epsilon_{n\ell} \phi_{n\ell}(r)$$

Note that one has a different equation for each of the $n\ell$ states (1s, 2s, sp ... etc.). The advantage of this scheme is that $\rho(r, T)$ is the self-consistent charge density profile already obtained from previous nonlinear screening calculations for the same density and temperature. Note that the continuum charge density $\rho_c(r, T)$ satisfies the requirement

$$\int \rho_c(\vec{r}, T) d\vec{r} = (z - 1)$$

Since $\rho(\vec{r}, T) = \rho_c(\vec{r}, T) + |\phi_{n\ell}(\vec{r})|^2$

and all $\phi_{n\ell}(r)$ are normalized to unity:

$$\int |\phi_n(\vec{r})|^2 d\vec{r} = 1$$

TABLE 1

Electronic Contribution to Equation of
State Pressure in Ryd/cm³

(The difference from ideal gas EOS shown in parenthesis)

Electron density (cm ⁻³)	Temperature (eV) →				
	0	0.0316	0.316	3.16	10
10 ²⁴	{ 2.003E24 (2.003E24)	{ 2.004E24 (2.002E24)	{ 2.006E24 (1.983E24)	{ 2.025E24 (1.793E24)	{ 2.275E24 (1.540E24)
10 ²³	{ 0.7074E23 (0.7074E23)	{ 0.7076E23 (0.7053E23)	{ 0.7085E23 (0.6853E23)	{ 0.8225E23 (0.590E23)	{ 1.142E23 (0.407E23)
10 ²²	{ 0.297E22 (0.297E22)	{ 0.299E22 (0.296E22)	{ 0.302E22 (0.279E22)	{ 0.443E22 (0.211E22)	{ 0.889E22 (0.154E22)
10 ²¹	{ 0.140E21 (0.140E21)	{ 0.155E21 (0.153E21)	{ 0.175E21 (0.151E21)	{ 0.321E21 (0.089E21)	{ 0.784E21 (0.049E21)
10 ²⁰	{ 0.067E20 (0.067E20)	{ 0.078E20 (0.076E20)	{ 0.095E20 (0.071E20)	{ 0.259E20 (0.027E20)	{ 0.750E20 (0.016E20)

TABLE 2

1s, 2s, 2p Energy Levels for a Neon Impurity in a Hydrogen Plasma at $T = 100$ eV for Three Different Electron Densities.

(The numbers in parenthesis show the percentage differences from corresponding Debye results. Units in Rydbergs.)

Electron Density (cm^{-3})	Potential Used in Eq. (II-8)	Bound States			Line Shift
		1s	2s	2p	
4.54×10^{24}	V_D	-72.816	-5.316	-4.076	6.260
	V_ξ	-75.499 (3.7%)	-6.623 (24.6%)	-5.560 (36.4%)	5.061
	V_{eff}	-78.695 (8.1%)	-7.383 (38.9%)	-6.591 (61.7%)	2.896
2.47×10^{24}	V_D	-79.369	-8.747	-7.939	3.570
	V_ξ	-80.605 (1.6%)	-9.487 (8.5%)	-8.759 (10.3%)	3.154
	V_{eff}	-82.800 (4.3%)	-9.930 (13.5%)	-9.330 (17.5%)	1.530
1.0×10^{24}	V_D	-86.482	-13.406	-13.022	1.540
	V_ξ	-86.842 (0.4%)	-13.668 (2%)	-13.302 (2.2%)	1.460
	V_{eff}	-88.043 (1.8%)	-14.037 (4.7%)	-13.781 (5.8%)	0.738

TABLE 3 (a)

Energy-Level Spectrum (Atomic Unit) for a Neon Impurity in a Hydrogen Plasma at $T = 200$ eV for Three Different Electron Densities.
 (Results of the self-consistent screening model discussed in the text are compared with corresponding Debye-screening results.)

Energy Levels	Electron Densities					
	$5 \times 10^{23} \text{ cm}^{-3}$		10^{24} cm^{-3}		$5 \times 10^{24} \text{ cm}^{-3}$	
	Self-Consistent	Debye	Self-Consistent	Debye	Self-Consistent	Debye
1s	-37.776	-45.151	-35.820	-43.244	-30.534	-35.809
2s	-5.836	-8.147	-4.691	-6.699	-1.635	-2.387
2p	-5.360	-8.045	-4.133	-6.508	-0.842	-1.731
3s	-1.166	-1.916	-0.563	-1.052		
3p	-1.005	-1.836	-0.388	-0.924		
3d	-0.795	-1.671		-0.653		
4s	-0.125	-0.301		-0.019		
4p	-0.070	-0.251				
4d		-0.149				
4f						

TABLE 3 (b)

Level Spectrum for an Argon Impurity Ion in a Hydrogen
 Plasma of Density 5×10^{23} Electrons/cm³ at a Temperature

T = 200 eV.

(Results obtained from the self-consistent screening model.)

Electron Density	Energy Levels (A.U.)									
	1s	2s	2p	3s	3p	3d	4s	4p	4d	4f
5×10^{23} cm ⁻³	128.17	21.556	19.932	5.807	5.297	4.702	1.579	1.374	1.104	0.778

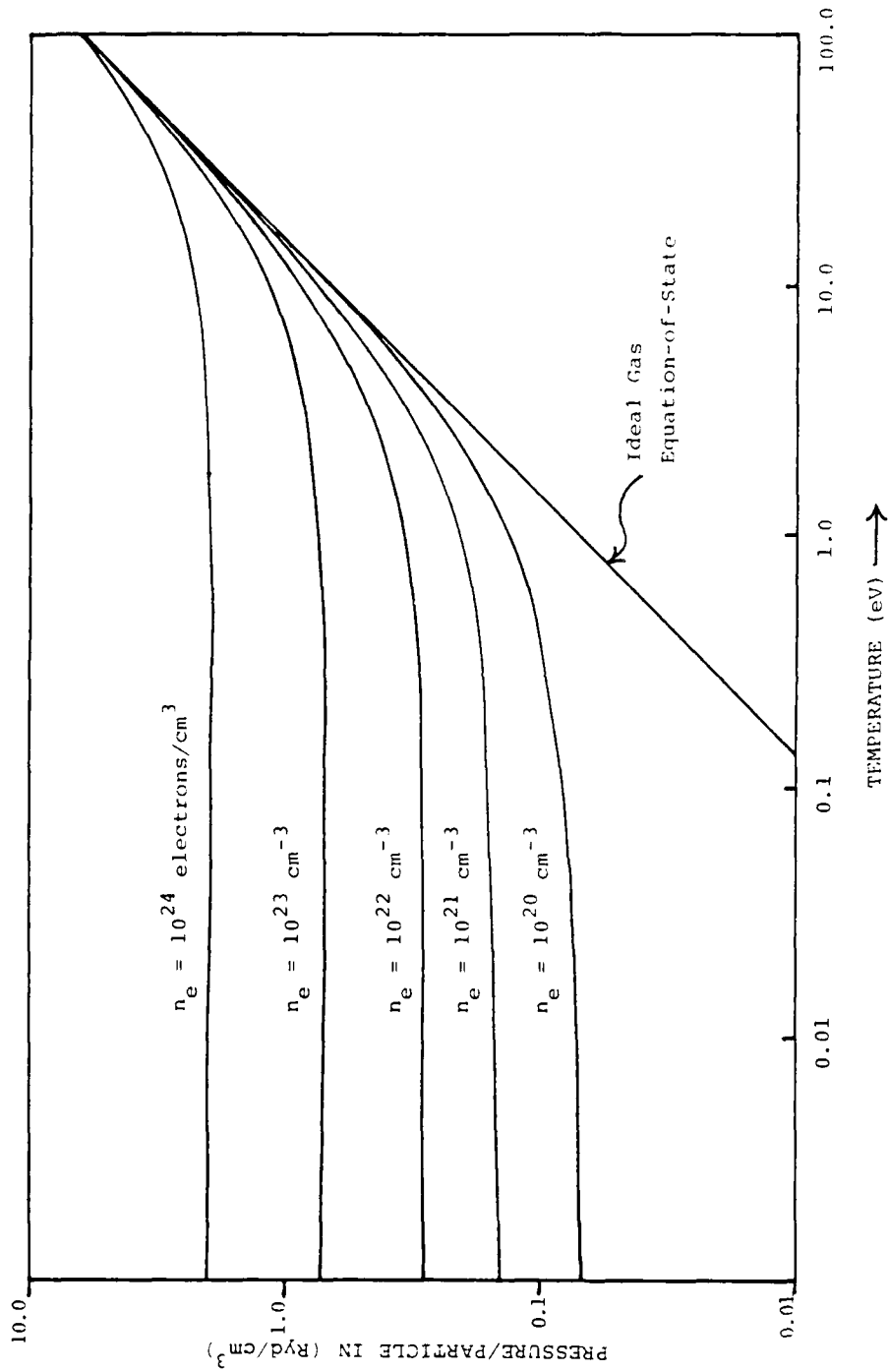


Figure 1. Electronic contribution to the Equation-of-State (EOS) in the temperature range 0-100 eV and the density range 10^{20} - 10^{24} electrons/cm³. Drastic differences from the ideal gas EOS are illustrated.

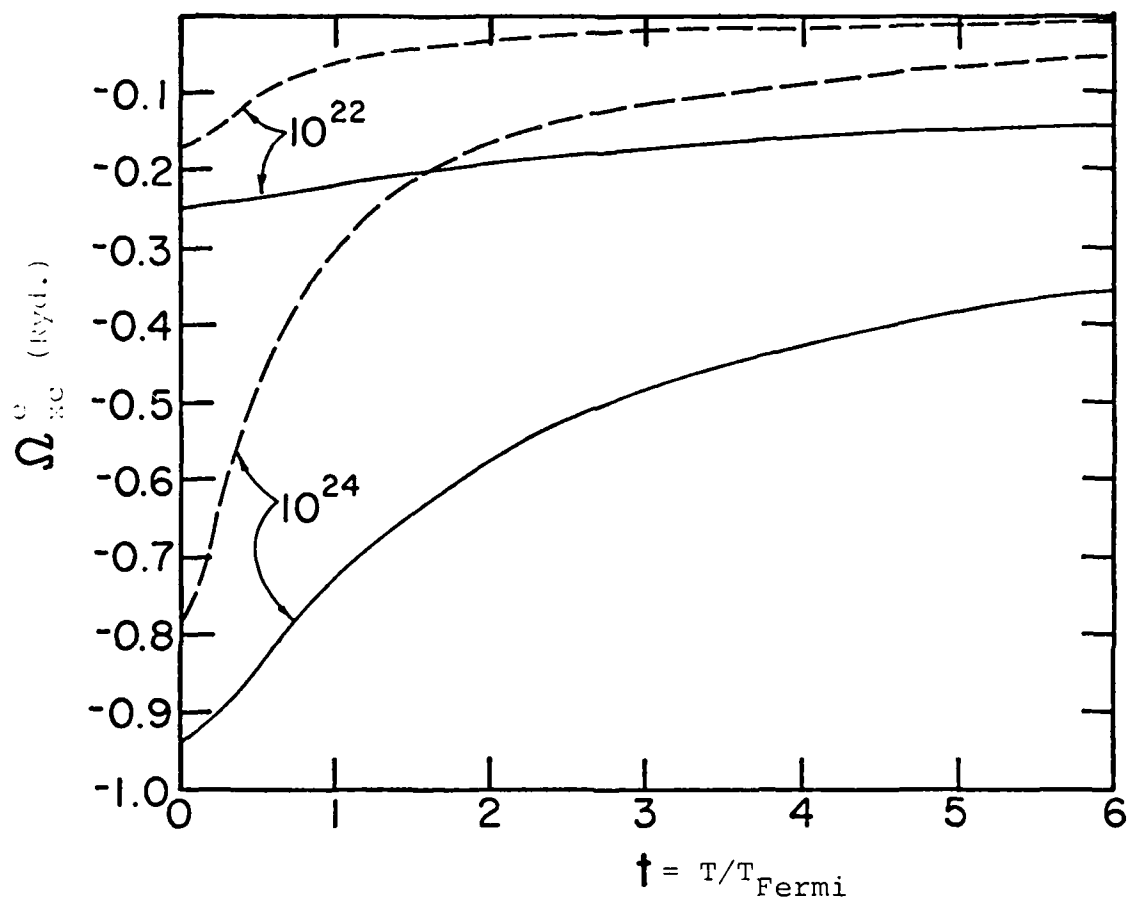


Figure 2. Total electronic exchange-correlation contribution to the thermodynamic potential Ω as a function of temperature for two different electronic densities. The dotted curve indicates the rapid decay of the exchange effect with increasing temperature. The high temperature part of Ω_{xc} is completely dominated by correlation effects.

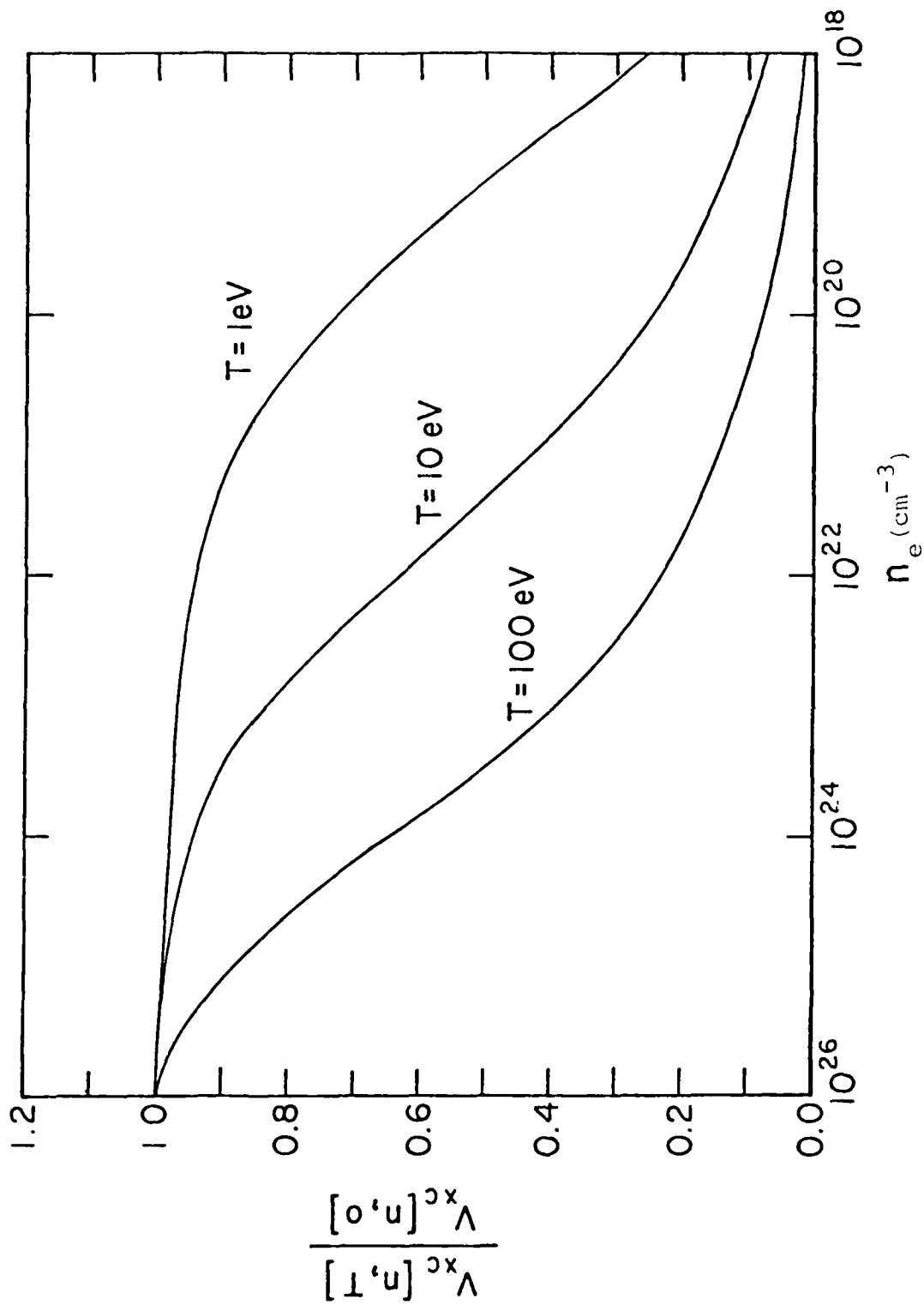


Figure 3. The exchange-correlation potential $V_{xc}[n, T]$ for electrons scaled by their zero temperature value $V_{xc}[n, 0]$ as a function of electron density at three typical plasma temperatures. This V_{xc} is used in the self-consistent calculations mentioned in the text.

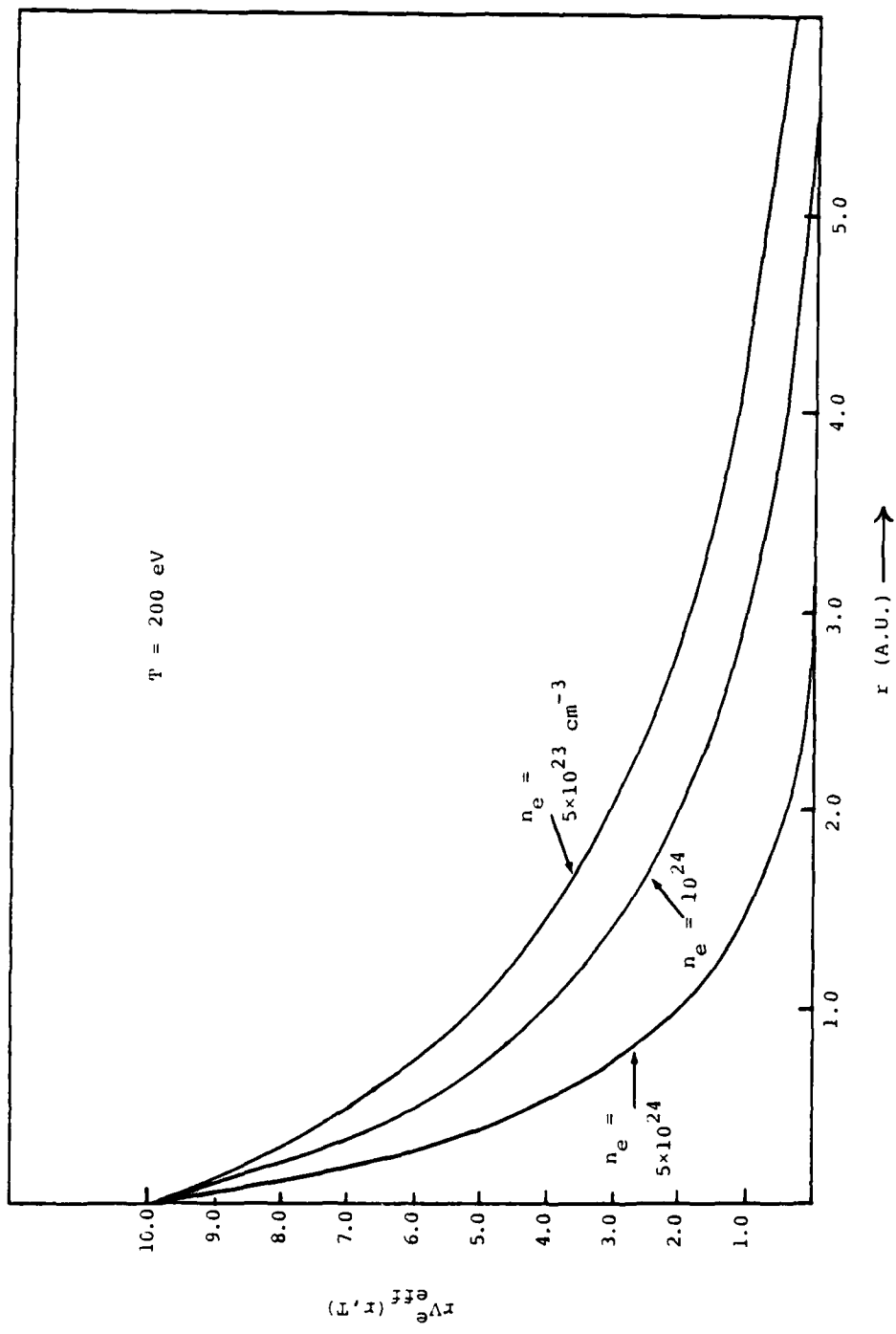


Figure 4. The strong density dependence of the self-consistent atomic potential Eq. (II-9) for a Neon ion embedded in a hydrogen plasma at $T = 200 \text{ eV}$.

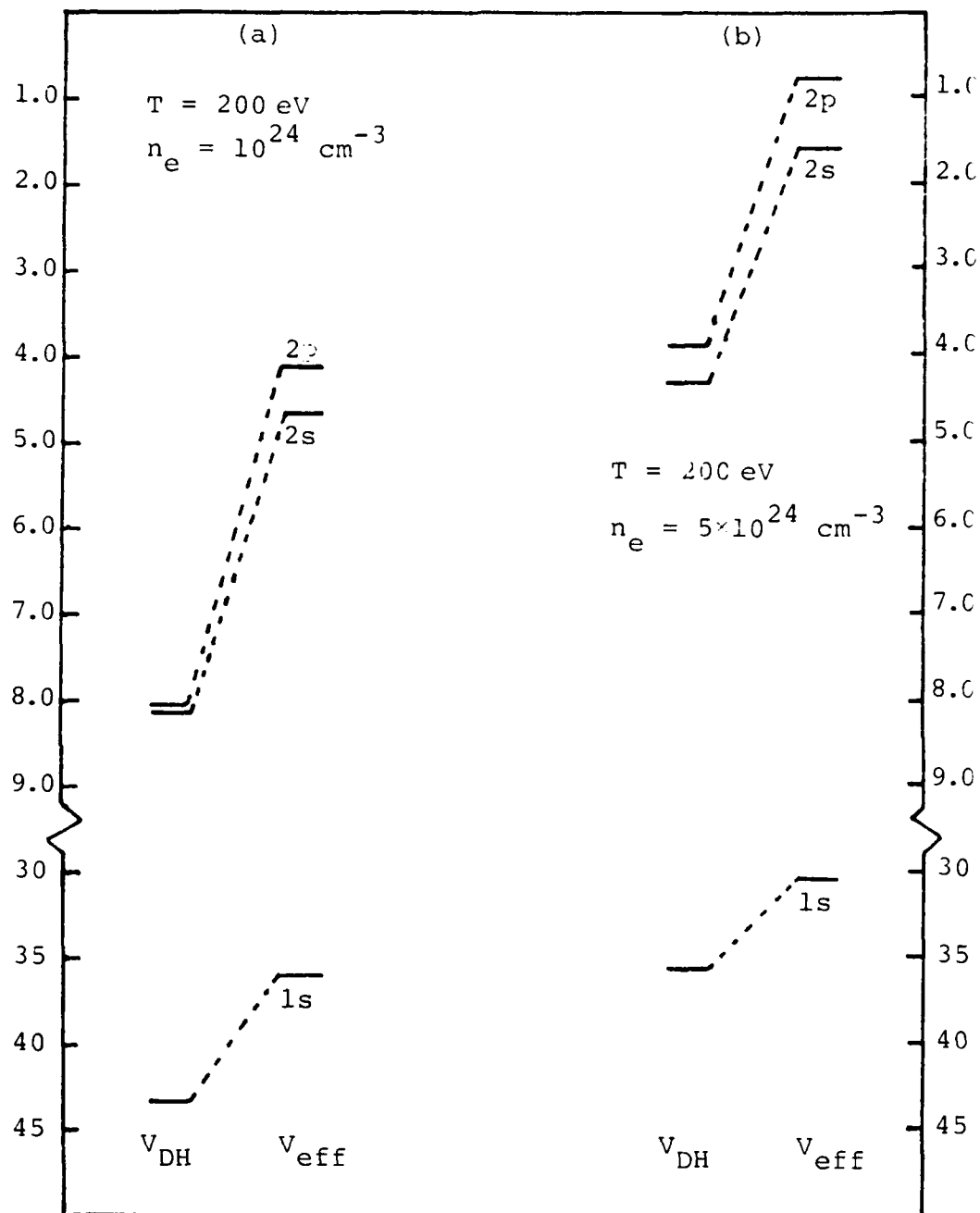


Figure 5. Energy-level spectrums for a Neon ion in a hydrogen plasma. Self-consistent results using V_{eff} yield drastic differences from the corresponding Debye spectrum. This emphasizes the importance of the nonlinear screening method used in our model.

DISTRIBUTION LIST

DEPARTMENT OF DEFENSE

Assistant to the Secretary of Def
Atomic Energy
ATTN: Military Applications
ATTN: Executive Asst

Defense Intelligence Agency
ATTN: DT-1B, R. Rubenstein

Defense Nuclear Agency
ATTN: RAAE
ATTN: STNA
ATTN: RAEE
2 cy ATTN: RAEV
4 cy ATTN: STTI/CA

Defense Tech Info Ctr
12 cy ATTN: DD

Field Command
DNA Det 1
Lawrence Livermore National Lab
ATTN: FC-1

Field Command
Defense Nuclear Agency
ATTN: FCPR
ATTN: FCTT
ATTN: FCTT, W. Summa
ATTN: FCTXE

Under Secy of Def for Rsch & Engrg
ATTN: Strar & Space Sys, OS

DEPARTMENT OF THE ARMY

Harry Diamond Labs
ATTN: DELHD-NW-RA, 22100
ATTN: DELHD-NW-P, 20240
ATTN: DELHD-NW-RI, Kervis 22900
ATTN: DELHD-TA-L, Tech Lib, 81100

US Army Nuclear & Chem Agency
ATTN: Library

US Army Test & Evaluation Comd
ATTN: DRSTE-CT-C

USA Missile Command
ATTN: Documents Section

DEPARTMENT OF THE NAVY

Naval Rsch Lab
ATTN: Code 4720, J. Davis
ATTN: Code 2000, J. Brown
ATTN: Code 4700, S. Ossakow
ATTN: Code 4770, G. Cooperstein
ATTN: Code 4701, I. Vitokovitsky

Naval Surface Weapons Ctr
ATTN: Code R40
ATTN: Code F31
ATTN: Code F34

Naval Weapons Center
ATTN: Code 343, FKA6A2, Tech Svcs

DEPARTMENT OF THE AIR FORCE

Air Force Weapons Lab
ATTN: NTYP
ATTN: CA
ATTN: NT
ATTN: SUL

Ballistic Missile Office, DAA
ATTN: ENSN

Dep Ch of Staff
Rsch, Dev and Acq
ATTN: AFRDQI

Space Division
ATTN: XP, Plans
ATTN: YEZ
ATTN: YGJ
ATTN: YKF
ATTN: YKS, P. Stadler
ATTN: YKM
ATTN: YNV

Strat Air Command
ATTN: XPFS
ATTN: DOTP

DEPARTMENT OF ENERGY

DEPARTMENT OF ENERGY
Attention Ofc of Inert Fusion
ATTN: C. Hilland
ATTN: T. Godlove
ATTN: S. Kahalas

OTHER GOVERNMENT AGENCY

Central Intelligence Agency
ATTN: OSWR/NED

DEPARTMENT OF ENERGY CONTRACTORS

University of California
Lawrence Livermore National Lab
ATTN: W. Pickles, L-401
ATTN: L. Wouters, L-47
ATTN: Tech Info Dept Lib
ATTN: L-153
ATTN: L-13, D. Meeker
ATTN: L-545, J. Nuckolls, Class L-53

Los Alamos National Lab
ATTN: MS222, J. Brownell

Sandia National Labs
ATTN: M. Clauser, Org 5241
ATTN: G. Kuswa, Org 5240
ATTN: Tech Lib 3141
ATTN: G. Yonas
ATTN: J. Powell
ATTN: D. Allen, Org 9336

DEPARTMENT OF DEFENSE CONTRACTORS

Advanced Rsch & Applications Corp
ATTN: R. Armistead

DEPARTMENT OF DEFENSE CONTRACTORS (Continued)

Aerospace Corp
ATTN: Library Acquisition M1/199
ATTN: V. Josephson
ATTN: S. Bower

BOM Corp
ATTN: Corporate Lib

BOM Corp
ATTN: L. Hoeft

soeing Co
ATTN: Aerospace Library

Berkeley Rsch Associates, Inc
4 cy ATTN: U. Gupta
4 cy ATTN: J. Orens

Dikewood Corp
ATTN: Tech Lib for D. Pirio

EG&G Wash Analytical Svcs Ctr, Inc
ATTN: Library

General Electric Co
ATTN: J. Peden
ATTN: H. O'Donnell

IRT Corp
ATTN: R. Mertz

JAYCOR
ATTN: E. Wenaas

JAYCOR
ATTN: R. Sullivan
ATTN: E. Alcaraz

Kaman Sciences Corp
ATTN: S. Face

Kaman Sciences Corp
ATTN: E. Conrad

Kaman Tempo
ATTN: DASIAC

Kaman Tempo
ATTN: Dasiac

Mission Rsch Corp
ATTN: B. Godfrey

Physics International Co
ATTN: C. Gilman
ATTN: G. Frazier
ATTN: C. Stallings

DEPARTMENT OF DEFENSE CONTRACTORS (Continued)

Lockheed Missiles & Space Co, Inc
ATTN: L. Chase

Lockheed Missiles & Space Co, Inc
ATTN: S. Taimuty

Maxwell Labs, Inc
ATTN: A. Kolb
ATTN: O. Cole
ATTN: D. Tanimoto
ATTN: A. Miller

McDonnell Douglas Corp
ATTN: S. Schneider

Mission Rsch Corp
ATTN: C. Longmire

Mission Rsch Corp
ATTN: V. Van Lint

Pacific-Sierra Rsch Corp
ATTN: L. Schlessinger
ATTN: H. Brode, Chairman SAGE

Pulse Sciences, Inc
ATTN: P. Spence
ATTN: I. Smith
ATTN: S. Putnom

R&D Associates
ATTN: P. Haas
ATTN: A. Latter

R&D Associates
ATTN: P. Turchi

Rand Corp
ATTN: P. Davis

Rand Corp
ATTN: B. Bennett

S-CUBED
ATTN: A. Wilson

Science Applications, Inc
ATTN: W. Chadsey
ATTN: M. Schmidt

Science Applications, Inc
ATTN: K. Sites

TRW Electronics & Defense Sector
ATTN: D. Clement
ATTN: Tech Info Ctr

END

FILMED

2-85

DTIC